Ilona Jastrzębska*, Szczerba Jacek and Stoch Paweł

Structural and Microstructural Study on the Arc-Plasma Synthesized (APS) $FeAl_2O_4$–$MgAl_2O_4$ Transitional Refractory Compound

DOI 10.1515/htmp-2015-0252
Received November 5, 2015; accepted April 11, 2016

Abstract: In this work, a pleonastic compound, a compound with a composition between hercynite and spinel *sensu stricto* $FeAl_2O_4$–$MgAl_2O_4$, was synthesized by a non-conventional method of arc-plasma synthesis (APS). The structure of the obtained spinel compound was characterized by means of X-ray diffraction and Mössbauer effect measurements. The microstructure was observed by applying scanning electron microscope (SEM)/energy dispersive spectrometer (EDS) method. It was found that the arc-plasma synthesized material was characterized by a monophasic character, a low-inversion parameter and a compact microstructure.

Keywords: hercynite, spinel, arc plasma synthesis, Mössbauer spectroscopy, XRD, SEM/EDS

Introduction

Compounds with a spinel structure, like hercynite or spinel *sensu stricto*, are today of great technological importance due to their beneficial physicochemical and mechanical properties, such as high melting points, corrosion resistance to Portland clinker and alkali environment, and thermal shock resistance, and because they can act as "substitutes" in the production of toxic chrome-containing refractories [1–4]. $FeAl_2O_4$ and $MgAl_2O_4$ are the examples of the spinel minerals rarely encountered in nature, and characterized by the high melting points of 1,780 °C and 2,135 °C, respectively [5], and low thermal expansion coefficients. They may form a complete solid solution, $Fe^{2+}/\sum(Mg^{2+} + Fe^{2+})$, with ratio ranging from 0.25 to 0.75 called pleonaste [6].

Hercynite ($FeAl_2O_4$) and regular (or true) spinel ($MgAl_2O_4$) belong to AB_2O_4 *sensu lato* oxide spinel group possessing the *Fd3m* symmetry (227 space group number). In the spinel crystal lattice all the divalent A^{2+} ions occupy 8a positions (1/8,1/8,1/8), whereas all of the trivalent Al^{3+} ions are placed in the 16d Wyckoff sites (1/2, 1/2,1/2), and oxygen ions O^{2-} are in 32e positions (1/4,1/4,1/4). Endmembers $FeAl_2O_4$ and $MgAl_2O_4$ are characterized by the normal cation distribution. This means that all of the divalent ferrous (Fe^{2+}) or magnesium Mg^{2+} ions occupy the tetrahedral (T_d) sites (the so-called A ... sites), while all of the Al^{3+} ions fill up the octahedral (O_h) ones (called as B sites) in the spinel unit cell [7], which is illustrated in Figure 1.

Nevertheless, such a distribution of cations is true but only for a low-temperature origin, because above the absolute temperature ions begin to exchange with their positions, where Fe^{2+}/Mg^{2+} cations begin to occupy O_h cavities, while Al^{3+} ions hop to T_d sites. Therefore, in practice at ambient conditions mixed spinels prevail. The introduced disorder, with contrast to the ordered end-member species, is described by the so-called inversion parameter x, which is the fraction of trivalent aluminium ions that passed from O_h to T_d sites [7]. This term was first introduced by Verwey and Heilmann [8]. Together with the lattice parameter a and the oxygen positional parameter u, they constitute parameters fully characterizing the spinel crystal structure. Worth mentioning here is the fact that inversion parameter x determines spinel type and takes values in range from 0 to 1 for the perfectly normal and inverse spinel, respectively. On the other hand, when the x parameter is between these values the spinel is partially inversed. And besides, random spinel is additionally distinguished by x equal to 2/3 [7].

Hercynite was reported to be found in the metallurgical slag as the product of reaction between refractories containing SiO_2 and iron melts with oxygen [9–11]. It was also observed in the slag when metallic Al was applied as

***Corresponding author: Ilona Jastrzębska,** Department of Ceramics and Refractories, Faculty of Materials Science and Ceramics, AGH University of Science and Technology, al. A. Mickiewicza 30, 30-059 Kraków, Poland, E-mail: ijastrz@agh.edu.pl
Szczerba Jacek, Stoch Paweł, Department of Ceramics and Refractories, Faculty of Materials Science and Ceramics, AGH University of Science and Technology, al. A. Mickiewicza 30, 30-059 Kraków, Poland

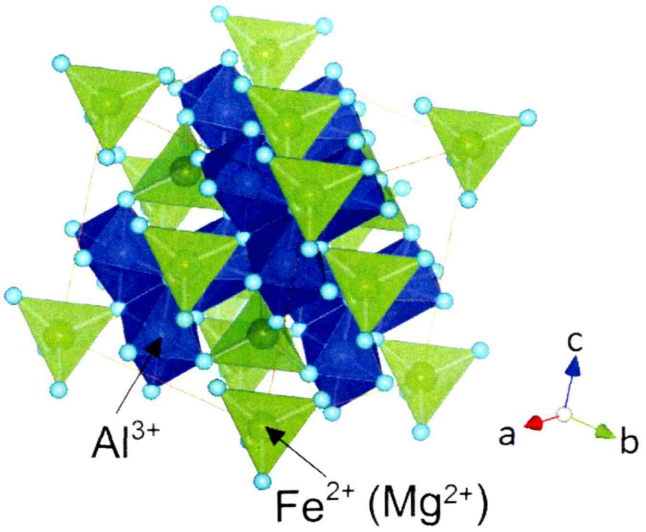

Figure 1: Structure of spinel, where green tetrahedrons represent [FeO_4] or [MgO_4], while the blue octahedrons denote [AlO_6] coordinates, and light blue balls refer to oxygen atoms.

the deoxidizer additive [12]. Moreover, the formation of $FeAl_2O_4$ was also reported by Okamoto et al. [13] in the intermediate layer occurring as the bonding interface in the process of joining of metal with alumina ceramics.

Hercynite, although not as popular as spinel [14–17], because of the difficulties encountered during its synthesis, possesses a great potential of the usefulness as the elastifying component of basic refractories. It was previously reported that addition of hercynite to MgO–$CaZrO_3$ material significantly improved its thermal shock resistance by a generation of microcracks that inhibited cracks propagation [18]. Moreover, Chenn et al. [19] investigated that hercynite facilitates formation of a protective coating on the refractory material in burning zone of cement rotary kiln during cement clinker production, which prevents the materials from premature damage.

Magnesia spinel materials were installed for the first time at 30 years of twentieth century and have been state of the art since the mid-1980s. Magnesia–hercynite materials have been developed only in the early 1990s of the same century and applied first in 1995 in cement rotary kiln [20, 21].

The ability of hercynite to interdiffuse with magnesia matrix, when it acts as a component of magnesia refractory material, makes the material more flexible by the local formation of secondary spinel phases, and therefore material is able to withstand thermal as well as mechanical strains, which constantly accompany the rotating kiln, and in result internal refractory lining [22]. The exchange of ions between hercynite and magnesia, or other material constituents, is of great interest, because by creating transitional spinel solid solutions or hybrid spinels [22] during the entire operational period they heal the cracks, which generate during the operation, and for this reason can be called as "intelligent materials". The interdiffusion with magnesia matrix is realized by the mutual exchange of ferrous/ferric ions with magnesium ones, which is possible due to the similarity in effective ionic radii [23] (Fe^{2+} = 0.063 nm, Fe^{3+} = 0.049 nm, Mg^{2+} = 0.057 nm, all values given for tetrahedral coordination).

Currently, materials prepared by using arc-plasma synthesis (APS) possess a great potential of applicability due to their high density, good corrosion resistance resulting from larger crystals formed and higher thermal stability [24].

Therefore, this method was applied for the synthesis of pure hercynite-spinel *sensu stricto* transitional compound (pleonaste), which was investigated in this work by means of structure and microstructure analysis.

Experimental

The starting reagents, which were reagents of high-grade powders of Fe_2O_3 and Al_2O_3 and MgO, were composed in the proportion expressed by the formula $Fe_{0.5}Mg_{0.5}Al_2O_4$ (pleonastic composition). Then, the starting powder mixture was pressed into the form of pellet of 20 mm in diameter with the pressure of 100 MPa. Subsequently, material was subjected to APS. The process of synthesis was carried out in *SpekoArc300* arc plasma furnace (Spaw-Projekt, Kraków, www.arc-furnace.pl) in a flow of the protective atmosphere of a noble gas, which was pure argon. In order to get a fully reacted and homogenized material, sample was melted twice. Owing to a non-contact spark ignition a risk of the sample pollution was avoided. The arc-plasma furnace was powered by an invertor source of power with the current regulation within the range of 10–300 A and equipped with a water-cooled copper crucible and a tungsten electrode.

The synthesized spinel material sample was subsequently powdered to the granulation below 0.063 mm and subjected to X-ray diffraction (XRD) analysis in order to identify its phase composition. The XRD measurement was conducted at ambient temperature, utilizing the PANalytical X'Pert Pro MPD X-ray diffractometer, in Bragg–Brentano geometry, with Cu-K_α radiation (λ = 1.54056 Å), in the 2θ range 5°–90°. The XRD pattern was processed applying Rietveld refinement as implemented in the Maud code [25].

Mössbauer spectroscopy (MS) measurement of the spinel material was conducted in a transmission mode by means of the RENON MsAa-3 spectrometer, equipped with the LND Kr-filled proportional detector and the He–Ne laser-based interferometer, which is used to calibrate a velocity scale. A commercial $^{57}Co(Rh)$ source kept at room temperature was applied for 14.41 keV resonant transition in ^{57}Fe. The obtained spectrum was fitted using Lorentzian shape line. The values of isomer shift (IS) were given relatively to α-Fe. The Mössbauer absorbers were prepared in a powder form.

The obtained material was observed under the ultra-high-definition Nova NanoSEM 200 scanning electron microscope (SEM) equipped with an energy dispersive spectrometer (EDS). The sample for the microscopic observations was both in the form of surface fracture and polished cross section prepared by the traditional ceramographic technique.

Results and discussion

XRD study

Figure 2 shows the refined XRD pattern for the APS spinel material. The all registered reflexes were characteristic for cubic spinel phase (space group *Fd3m*). The spinel crystal lattice parameter was determined on $a = 8.1148(2)$Å, while the oxygen positional parameter equalled $u = 0.2600$. In comparison to pure hercynite spinel [26], which lattice and oxygen parameter were previously estimated as $a = 8.1320(9)$Å and $u = 0.262$, respectively, the values obtained in this study for mixed spinel are decreased. Simultaneously, they are increased with respect to parameters for spinel *sensu stricto* synthesized by flux growth method. The XRD pattern was refined by means of Rietveld method and using XRD data for $Fe_{0.494}Mg_{0.544}Al_{1.962}O_4$ obtained by Andreozzi and Lucchesi [27], and with the attained parameters $R_w = 9.0321\,\%$ and sigma = 1.0124, confirming a satisfactory fitting procedure.

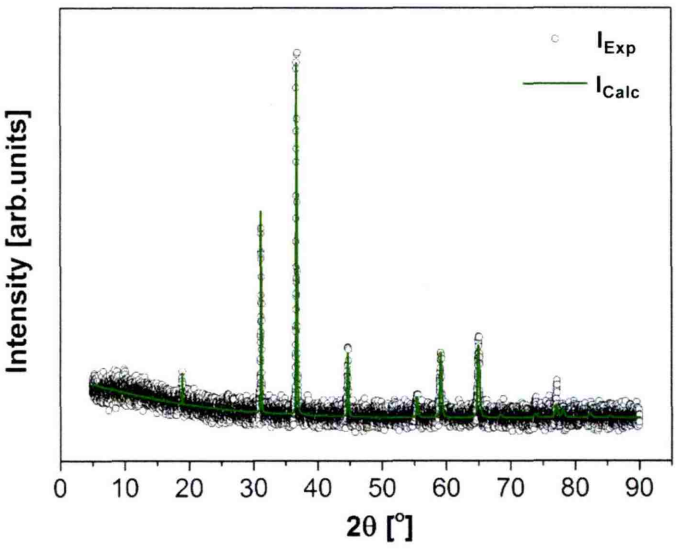

Figure 2: The refined XRD pattern of the arc-plasma synthesized spinel compound.

Mössbauer effect study

In order to fully characterize the spinel crystal structure by determining its inversion parameter *x*, the Mössbauer spectroscopy (MS) measurement was performed. The obtained ambient temperature Mössbauer spectrum is illustrated in Figure 3.

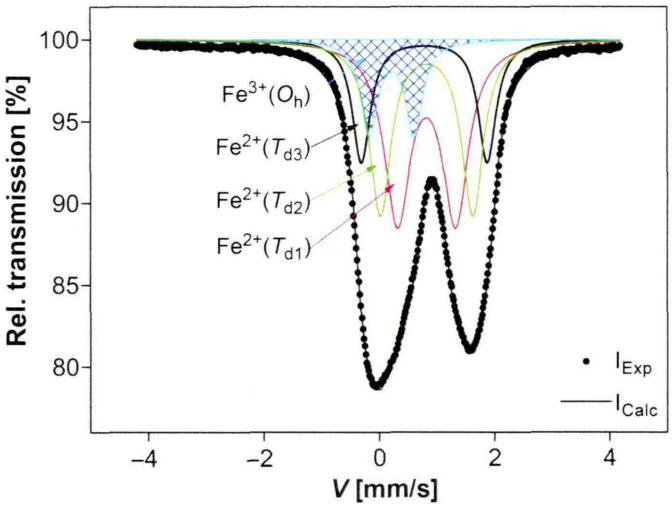

Figure 3: The Mössbauer spectrum at ambient temperature of the arc-plasma synthesized pleonaste spinel.

The fitted continuous spectrum (corresponding to the experimental points) was resolved into four subspectra that were described in the plot. As it can be observed, there are ferrous (Fe^{2+}) and ferric (Fe^{3+}) ions in the spinel structure [28], which was determined based on the obtained IS values. Moreover, they occupy different positions in the spinel crystal lattice. The average value of the IS for the Fe^{2+} ions was 0.910 mm/s, while for the Fe^{3+} ones it was estimated as 0.321 mm/s. Besides, it was found that divalent iron is distributed among the tetrahedral positions of different symmetry, with the mostly

distorted T_{d3} one, which was characterized by the highest quadrupole splitting (QS) value of 2.181(10) mm/s, whereas for the rest ones it was equal to 1.601(7) mm/s (T_{d2}) and 1.011(10) mm/s (T_{d1}). The component of the lowest relative area and hyperfine parameters of IS = 0.320(4) mm/s and QS = 0.776(7) mm/s (marked by blue colour in Figure 3) were attributed as responsible for the octahedrally coordinated Fe^{3+} ions.

Additionally, it was found that the ratio of the percentage surface area for Fe^{2+}/Fe^{3+} was in proportion of 85:15. Based on the obtained area ratio and assuming that all the magnesium ions occupy tetrahedral sites, due to their high site preference energy in T_d positions [29], the chemical formula of the synthesized spinel material was established as follows (eq. (1)):

$$\left(Fe^{2+}{}_{0.425}Mg_{0.5}Al_{0.075}\right)^{T_d}\left(Fe^{3+}{}_{0.038}Al_{0.949}\square_{0.013}\right)_2{}^{O_h}O_4. \quad (1)$$

where indices T_d and O_h denote tetrahedral and octahedral coordinations, respectively and square designates an ion vacancy.

Taking under consideration the surplus of the positive charge at the tetrahedral site, the presence of vacancies at O_h sites was reflected in the chemical formula to account for charge balance. The preference of vacancies occupation in the octahedral positions of spinel lattice was stated in Ref. [30]. The established chemical formula of the investigated spinel compound shows that its inversion parameter is equal to $x = 7.5\,\%$ and is much lower than x for pure hercynite which was reported to be $x = 23\,\%$ [26]. Such a decline in the inversion parameter value with the exchange of iron by magnesium ions is probably associated with the high-site preference energy of Mg^{2+} in T_d cavities, which prevent aluminium ions against passing from O_h to T_d sites.

SEM/EDS study

Figure 4(a) and (b) shows SEM images taken with the use of BSED mode for the cross-sectional sample (Figure 4(a)), and applying LVD (Low Vacuum Detector) mode for the fracture surface (Figure 4(b)), both in magnification of 1,000×.

It can be observed from the image of the cross section of the spinel sample that there are light- and dark-grey regions, especially able to distinguish on the right side of the image. The first ones prevail in the vicinity of the zig-zag-like cracks, which constitute boundaries between spinel crystals. On the other hand, inside of these crystals are visible by dark-grey colour. The observed microregions were examined by EDS in points 1 and 2, marked in Figure 3(a). The elemental composition measured in points 1 and 2 was as follows: point 1: Fe-12.2 %, Mg-4.2 %, Al-32.4 %, O-51.2 %; point 2: Fe-3.9 %, Mg-11.3 %, Al-33.8 %, O-51.0 %. So, light-grey regions are enriched with iron atoms, while dark-grey areas are enriched with aluminium atoms, with respect to approximate stoichiometry of spinel compound. The ratio of Al/(Fe + Mg) in point 1 equals 2, which is in compliance with the composition of stoichiometric spinel, while in point 2 it slightly increased to the value of 2.2.

The observed difference in the content of Fe atoms in points 1 and 2 (Figure 4(a)) was probably the effect of the diffusion of iron atoms from the higher temperature zone (point 2) to the lower temperature zone (point 1: boundaries between the crystals), as a result of temperature gradient across the crystal.

The morphology of the APS material, exhibited in Figure 4(b), is revealed by the small crystals that grew from the larger massive ones. The microstructure is rather dense and well compacted with the sparsely occurring voids. The image of the fracture surface does not allow

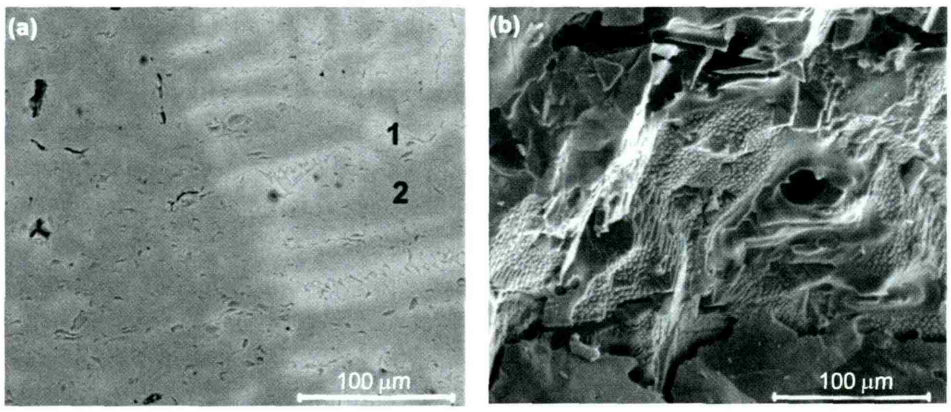

Figure 4: SEM images of the investigated spinel material: (a) polished cross section and (b) fracture surface.

the microregions with the chemical gradient to be distinguished, as it was observed for the cross-sectional sample.

Conclusions

The pleonastic Fe(50 %)Mg(50 %) aluminate spinel was synthesized in this work by the non-conventional method for the synthesis of ceramic compounds (APS) and investigated in view of its structure and microstructure.

The APS method permitted to obtain the monophasic spinel compound, confirmed by the XRD analysis, with the low inversion parameter of $x = 7.5\,\%$ determined by means of the Mössbauer effect measurement. The microstructure of the obtained material was compact, with sparsely occurring voids.

It was found that iron atoms tend to diffuse in the direction of outside crystal surfaces that constitute lower temperature zones.

The obtained results showed that it is possible to produce, in a fast route (by APS method), the material of pleonastic composition, which can be applied as the effective and good quality addition to refractory materials, for example in cement rotary kiln.

Acknowledgements: This work was supported by the statutory funds of the Faculty of Materials Science and Ceramics AGH in Kraków.

References

[1] F. Baruthio, Biol. Trace Elem. Res., 32 (1992) 145–153.
[2] L. Guangpink, L. Nan, Y. Wen, G. Changhe, Z. Wei and L. Yuanyuan, Ceram. Int., 40(6) (2014) 8149–8155.
[3] E. Rodíguez, G.A. Castillo, J. Contreras, R. Puente-Ornelas, J.A. Aguilar-Martínez, L. García and C. Gómez, Ceram. Int., 38 (2012) 6769–6775.
[4] G. Gelbmann, R. Krischanitz and S. Jörg, RHI Bull., 2 (2013) 10–12.
[5] C.A. Schach, Refractories Handbook, Marcel Dekker, New York (2004).
[6] W.A. Deer, R.A. Howie and J. Zussman, An Introduction to the Rock-Forming Minerals, Longman Scientific & Technical, Harlow, England (1992), p. 695.
[7] K.E. Sickafus, J.M. Wills and N.W. Grimes, J. Am. Ceram. Soc., 82(12) (1999) 3279–3292.
[8] E.J.W. Verwey and E.L. Heilmann, J. Chem. Phys., 15(174) (1947) 174–180.
[9] T. Zienert and O. Fabrichnaya, J. Europ. Ceram. Soc., 35 (2015) 1317–1326.
[10] E. Kapilashrami, V. Sahajwalla and S. Seetharaman, Proceedings of the VII International Conference on Molten Slags Fluxes and Salts, Johannesburg (2004), pp. 417–422.
[11] E. Kapilashrami, V. Sahajwalla and S. Seetharaman, J. Mat. Sci., 40 (2005) 2371–2375.
[12] K. Wasai, K. Mukai, H. Fuchiwaki and A. Yoshida, ISIJ Int., 39(8) (1999) 760–766.
[13] I. Okamoto, M. Naka and K. Asami, Trans. JWRI, 11 (1982) 131–133.
[14] P. Biswas, K. Rajeswari, V. Mahendar and R. Johnson, Ceram. Int., 39 (2013) 9819–9821.
[15] I. Reimanis and H.J. Kleebe, J. Am. Ceram. Soc., 92(7) (2009) 1472–1480.
[16] R. Salomao, M.O.C. Villas Bôas and V.C. Pandolfelli, Ceram. Int., 37 (2011) 1393–1399.
[17] J. Szczerba, I. Jastrzębska, Z. Pędzich and M.M. Bućko, J. Mat. Sci. Chem. Eng., 2 (2014) 16–25.
[18] E.A. Rodríguez, A.K. Limones, J.E. Contreras, J.J. Ruiz-Valdés, R. Puente-Ornelas, A.M. Arato and J.A. Aguilar-Martínez, J. Eur. Ceram. Soc., 35 (2015) 2631–2639.
[19] J. Chenn, M. Yan, J. Su, B. Li and J. Sun, Ceram. Int., 42(1) (2016) 569–575.
[20] M. Geith, C. Majcenovic and A. Wiry, RHI Bull., 1 (2003) 25.
[21] R. Krischanitz. 20 Years Hercynite Technology. Website access in 27.08.2015: http://www.rhi-ag.com/linkableblob/internet_en/74150/data/Magnesia_Hercynit_Art-data.pdf
[22] G. Liu, N. Li, W. Yan, G. Tao and Y. Li, J. Ceram. Proc. Res., 13(4) (2012) 480–485.
[23] R.D. Shannon, Acta Cryst. A, 32 (1976) 751–767.
[24] I. Jastrzębska and J. Szczerba, Proceedings of the X Krakow Conference of Young Scientists, Krakow (2015), pp. 9–10.
[25] L. Lutterotti, S. Matthies and H.R. Wenk, Proceedings of the 17th International Conference on Textures of Materials ICOTOM 12, Montreal (1999).
[26] I. Jastrzębska, J. Szczerba, P. Stoch, A. Błachowski, K. Ruebenbauer, R. Prorok and E. Śnieżek, Nukleonika (J. Nucl. Res.), 60(1) (2015) 45–47.
[27] G.B. Andreozzi and S. Lucchesi, Am. Miner., 74 (1989) 339–351.
[28] I. Dézsi, I. Szűcs and E. Sváb, J. Radioanal. Nucl. Chem., 246(1) (2000) 15–19.
[29] A. Navrotsky, C. Ma, K. Lilova and N. Birkner, Science, 330 (2010) 199–201.
[30] R. Dupree, M.H. Lewis and M.E. Smith, Phil. Mag. Lett., 53(2) (1986) L17–L20.